Targeting the Inverted CCAAT Box 2 in the Topoisomerase IIα Promoter by **JH-37**, an Imidazole−Pyrrole Polyamide Hairpin: Design, Synthesis, Molecular Biology, and Biophysical Studies†

James A. Henry,‡ N. Minh Le,‡,§ Binh Nguyen,§ Cameron M. Howard,‡ Suzanna L. Bailey,‡ Sarah M. Horick,‡ Karen L. Buchmueller,‡ Minal Kotecha,|| Daniel Hochhauser,|| John A. Hartley,|| W. David Wilson,*,§ and Moses Lee*,‡

Department of Chemistry, Furman University, Greenville, South Carolina 29613, Department of Chemistry, Georgia State University, Atlanta, Georgia 30303, and Department of Oncology, Royal Free and University College Medical School, London W1W 7BS, U.K.

Received June 10, 2004; Revised Manuscript Received July 28, 2004

ABSTRACT: The topoisomerase IIα promoter is regulated through transcription factor interactions with five inverted CCAAT boxes (ICBs). In confluent cancer cells, binding of nuclear factor Y to ICB2 represses the expression of this gene, contributing to resistance to topoisomerase II poisons. The ICB sites within the topoisomerase IIα promoter are, therefore, potential targets for the design of anticancer drugs and gene control agents. The synthesis and DNA binding properties of a hairpin polyamide molecule (**JH-37**) that targets 5′-TTGGT-3′ found in ICB2 and ICB3 sites are described. Gel shift and DNase I footprinting studies on the topoisomerase IIα promoter showed **JH-37** to preferentially bind to ICB2,3 and ICB1 sites. The larger ΔT_M values for ICB2,3 (8−9 °C) over ICB1,4,5 (4−5 °C) indicated a preference of **JH-37** for ICB2,3. CD titration studies confirmed the binding of **JH-37** to the minor groove, with a 1:1 binding stoichiometry. Results from SPR studies showed **JH-37** to bind most strongly to ICB2 ($K = 3 \times 10^7$ M^{-1}), followed by ICB1, the non-ICB sequence (TGCA), and finally the ICB mutant (ICB2m). The improved binding to ICB2 is largely due to a lower dissociation rate of the compound at the preferred site. To our knowledge, this is the first example on the use of SPR for studying the interactions of hairpin polyamides with DNA. Binding of **JH-37** to ICB2 was corroborated by ITC studies, in which the $\Delta G°$ of binding is driven by both enthalpy and entropy. With knowledge of the fundamental thermodynamic and kinetic properties that govern the molecular recognition of polyamides with DNA, we are poised to systematically edit the structure of **JH-37** in order to further enhance its binding affinity and selectivity for ICB2,3. Our strategy for designing molecules that control gene expression is to target shorter, but multiple, binding sites that are in close array within the promoter. Binding of **JH-37** to multiple ICB sites in the topoisomerase IIα promoter is an ideal test for this strategy. This approach is in contrast to the traditional strategy of targeting 15−16 base pairs, which has not been successful in actual biological systems due to poor cell uptake and distribution.

The expression of topoisomerase IIα (topoIIα)[1] is a determinant of response to chemotherapeutic agents including etoposide and doxorubicin (*1*). Confluent cells may downregulate expression of the topoIIα gene, and this may contribute to resistance to these agents (*1*−*3*). The topoII poisons etoposide and doxorubicin interact with the cleavable ternary enzyme/DNA complex with formation of protein-associated DNA double strand breaks leading to the onset of apoptosis (*4*, *5*).

The topoIIα promoter from human cells has been sequenced and characterized (*1*). Several consensus elements are found in the promoter, including two GC boxes (potential SP1 binding sites) and five inverted CCAAT boxes (ICB). Results from molecular cloning, mutation, and reporter assay studies identified the critical control element in confluence-induced downregulation as ICB2, located between −144 and −101 sites from the gene. Isaacs and co-workers (*1*) discovered that NF-Y, a nuclear protein, binds to this ICB site and bends the DNA by 62−68° (*6*).

On the basis of the NF-Y/ICB model for downregulating the expression of the topoIIα gene in confluent cells, Tolner and co-workers suggested that confluence-arrested cancer cells could be resensitized to topoIIα drugs by inhibiting the binding of NF-Y to ICB2 (*2*). Using a series of minor

† This work was supported by the NSF (REU), The Henry and Camille Dreyfus Foundation, and the Research Corporation.

* To whom correspondence should be addressed. M.L.: tel, (864) 294-3368; fax, (864) 294-3559; e-mail, Moses.Lee@furman.edu. W.D.W.: tel, (404) 651-3903; e-mail, chewdw@panther.gsu.edu.

‡ Furman University.

§ Georgia State University.

|| Royal Free and University College Medical School.

[1] Abbreviations: ICB, inverted CCAAT box; SPR, surface plasmon resonance; ITC, isothermal titration calorimetry; CD, circular dichroism; NF-Y, nuclear factor Y; RU, response unit; ODN, oligodeoxyribonucleotide; topoIIα, topoisomerase IIα.

10.1021/bi048785z CCC: $27.50
Published on Web 09/03/2004

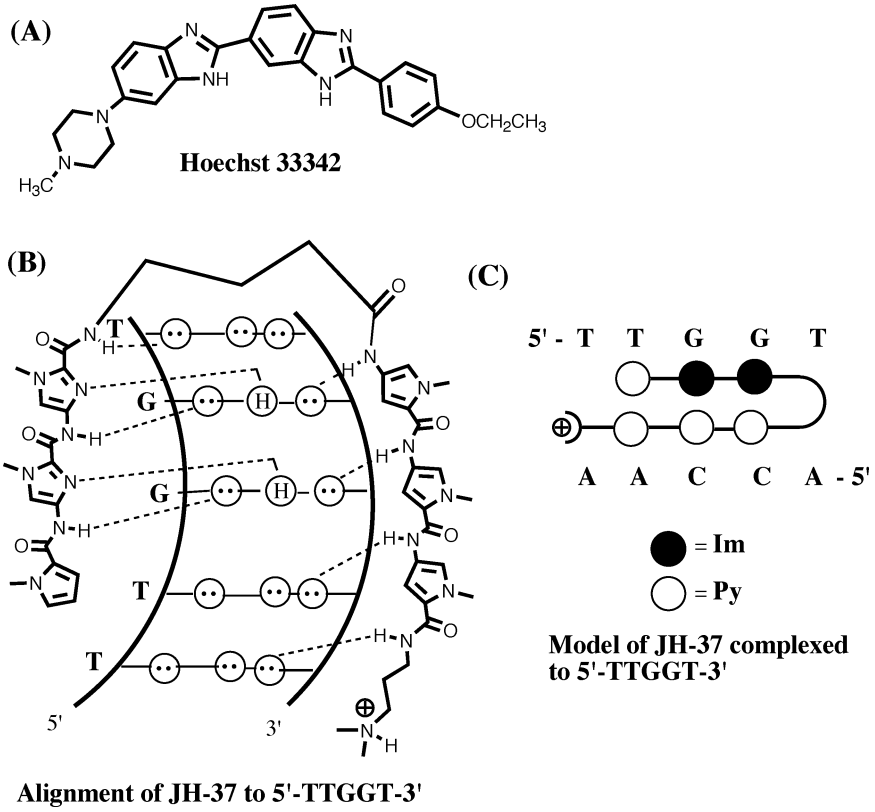

FIGURE 1: (A) Structure of Hoechst 33342. (B, C) Structure and model for recognition of **JH-37** for the 5′-TTGGT-3′ sequence. The stacked heterocyclic system recognizes 5′-(A·T)GG sequences.

groove and sequence-specific binding agents, the researchers found that Hoechst 33342 (Figure 1A), which binds to AT-rich sequences including binding to ICB1 and ICB2, was able to upregulate the transcription of topoIIα in confluent cells. These upregulated cells were found to be sensitive to the cytotoxic action of topoIIα drugs, such as etoposide (*2*). The findings suggested that ICB sequences within the promoter could be a potential target for sequence-specific minor groove agents able to inhibit NF-Y binding. Even though Hoechst 33342 was able to sensitize confluent cells to etoposide, it is not clinically useful due to its multiple modes of action and lack of sequence specificity. Consequently, to overcome the resistance of confluent cancer cells to topoIIα acting drugs, there could be therapeutic use for molecules that exhibit specificity for binding to ICB2.

In addition to controlling the expression of the topoIIα promoter, ICB sites are found in many gene promoters (*7*), including the human *mdr1* gene (*8*, *9*). Binding of NF-Y to the ICB site within the *mdr1* promoter upregulates transcription of the gene and elevates the level of P-glycoprotein in multidrug-resistant cancer cells (*10*). Inhibition of the binding of NF-Y in MDR cancer cells could, therefore, sensitize cells to chemotherapy. Consequently, the ability to control the expression of specific genes would be useful in several contexts (*11*).

Our strategy for designing compounds capable of binding to ICB2, which has the sequence 5′-ATTGGT-3′ (*1*), is based on a class of polyamide hairpins that are analogues of distamycin, a minor groove and A·T sequence selective binding agent. In recent years, Dervan and co-workers (*12*, *13*), Lown and co-workers (*14*), and Lee and co-workers (*15*−*17*) have systematically investigated the DNA sequence specific recognition of polyamide analogues. These imidazole- and pyrrole-containing polyamides were found to form stacked side-by-side dimers in an antiparallel fashion, and they interacted tightly within the minor groove. It is well-established that a stacked pyrrole/pyrrole pair binds to an A·T or T·A, a pyrrole/imidazole pair binds preferentially to C·G, a imidazole/pyrrole pair binds selectively to G·C, and an imidazole/imidazole pair binds to G·C or C·G. Dervan's group has also demonstrated that conjugates of polyamides that contain a γ-aminobutyrate linker are capable of folding and forming hairpin structures. In the hairpin conformation, the polyamides could essentially form intramolecular stacked dimers and exhibit high DNA binding affinity and sequence selectivity. Using the rules of DNA sequence recognition for polyamides, our laboratories have developed a novel γ-hairpin, **JH-37** (Figure 1B), for binding to the 3′-flanking sequence (5′-TTGGT-3′) of ICB2 and ICB3 sites. Models for the binding of **JH-37** to this sequence are depicted in Figure 1B,C.

This paper describes the synthesis of **JH-37**, as well as its ability to selectively bind to ICB2 and ICB3. The DNA binding properties were characterized by molecular biology (electrophoretic mobility shift assay, or EMSA, and DNase I footprinting) and biophysical experiments [DNA melting, CD, surface plasmon resonance (SPR), and isothermal titration calorimetry (ITC)].

EXPERIMENTAL PROCEDURES

*Synthesis of **JH-37**.* A solution of *N*-(*N*′,*N*′-dimethylaminopropyl)-1-methyl-4-[1-methyl-4-(1-methylpyrrole-2-carboxamido)pyrrole-2-carboxamido]imidazole-2-carboxamide (**6**) (139 mg, 0.279 mmol) in cold methanol (30 mL) was hydrogentated over 5% Pd on carbon (70 mg) at room

temperature and atmospheric pressure for 3 h, at which time TLC analysis indicated complete reduction of starting material. The catalyst was removed by filtration. The filtrate was concentrated, and the residue was coevaporated with dry CH_2Cl_2 (10 mL, twice) to give an amine product, **7**, which was unstable and thus kept under high vacuum until used directly in the next step.

A mixture of carboxylic acid **5** (153 mg, 0.335 mmol) and PyBOP (175 mg, 0.335 mmol) was suspended in freshly distilled and dry CH_2Cl_2 (100 mL). A solution of the amine from the above reduction reaction in dry CH_2Cl_2 (15 mL) was added to the suspension. The reaction mixture was stirred for 10 min, at which time dry *N*,*N*-diisopropylethylamine (0.122 mL, 0.698 mmol) was added. The color of the reaction solution turned from a cloudy yellow to clear yellow. The reaction solution was allowed to stir at room temperature under N_2 atmosphere for 2 days. TLC analysis at this point indicated that the reaction had proceeded very slowly. Thus, additional amounts of PyBOP (87.0 mg, 0.167 mmol) and DIPEA (0.25 equiv, 0.061 mL, 0.349 mmol) were added to the reaction flask. The reaction was allowed to stir for an additional 2 h. The reaction solution was then basified using 3 M sodium hydroxide until the pH level was greater than 10. The organic layer was extracted with $CHCl_3$ and EtOAc, individually. The organic layers collected were combined, dried with Na_2SO_4, gravity filtered, and concentrated to yield a light brown oil which was purified on a silica gel column (eluent: 5−45% MeOH/ $CHCl_3$). The desired fractions were collected and concentrated to give the desired product as a yellow solid (93.6 mg, 0.103 mmol, 37%), mp 154−162 °C. TLC (15% MeOH/$CHCl_3$) R_f 0.075. IR (neat): 3389, 2963, 2919, 2857, 2359, 1652, 1536, 1470, 1261. UV (water): 312 (ϵ = 56800 M^{-1} cm^{-1}). ^1H NMR (500 MHz, DMSO-d_6): 10.35 (s, 1H), 9.88 (s, 1H), 9.86 (s, 1H), 9.82 (s, 1H), 9.37 (s, 1H), 8.25 (t, 5.5, 1H), 8.05 (t, 4.0, 1H), 7.62 (s, 1H), 7.51 (s, 1H), 7.24 (d, 1.6, 1H), 7.17 (d, 1.6, 1H), 7.14 (d, 1.5, 1H), 7.12 (d, 1.6, 1H), 7.11 (d, 1.5, 1H), 7.02 (d, 1.2, 1H), 6.99 (t, 1.2, 1H), 6.86 (d, 1.5, 1H), 6.81 (d, 1.5, 1H), 4.00 (s, 3H), 3.95 (s, 3H), 3.88 (s, 3H), 3.83 (s, 3H), 3.82 (q, 6.0, 2H), 3.81 (s, 3H), 3.78 (s, 3H), 3.18 (q, 6.0, 2H), 2.27 (t br, 6.5, 4H), 2.15 (s, 6H), 1.81 (quintet, 6.5, 2H), 1.61 (quintet, 6.5, 2H). TOF-MS (electrospray) *m*/*z* (relative intensity): 907 ($M + H^+$, 40). HRMS (TOF) for $C_{43}H_{55}N_{16}O_7$ ($M + H^+$): calcd, 907.4440; obsd, 907.4464.

DNase I Footprinting. A radiolabeled probe of 479 bp corresponding to positions −489 through −10 relative to the transcriptional start site of the topoisomerase IIα promoter was generated using a radiolabeled primer in a polymerase chain reaction as previously described (*4*). DNase I footprint reactions were performed by incubating 0.1 ng of the probe with either **JH-37** alone or with 30 μg of nuclear extract at room temperature for 2 h. Subsequently, 1 unit of DNase I (Promega) was added, the digestion was allowed to occur for 3 min, and the reaction was stopped by adding 30 mM K-EDTA, 200 mM NaCl, and 1% SDS. Samples were purified by phenol−chloroform treatment and alcohol precipitation. The resulting pellets were resuspended in loading buffer containing formamide and heat-denatured at 95 °C for 3min. Denaturing polyacrylamide gels (6%) (Sequagel; National Diagnostics) were used for separation, and dried gels were exposed to Kodak X-Omat-LS film at −80 °C.

DNA Denaturation Experiments. The synthetic oligonucleotides used in these studies were obtained from Qiagen, and they are as follows: ODN 1, ICB1 5′-flank, 5′-CAG GGA TTG GCC TTTTT GGC CAA TCC CTG; ODN 2, ICB1 3′-flank, 5′-GGA TTG GCT GGC TTTTT GCC AGC CAA TCC; ODN 3, ICB2 5′-flank, 5′-CTA CGA TTG GTC TTTTT GAC CAA TCG TAG; ODN 4, ICB2 3′-flank, 5′-CGA TTG GTT CTC TTTTT GAG AAC CAA TCG; ODN 5, ICB3 5′-flank, 5′-ACC TGA TTG GTC TTTTT GAC CAA TCA GGT; ODN 6, ICB3 3′-flank, 5′-GGA TTG GTT TAC TTTTT GTA AAC CAA TCC; ODN 7, ICB4 5′-flank, 5′-GTC TCA TTG GCC TTTTT GGC CAA TGA GAC; ODN 8, ICB4 3′-flank, 5′-GCA TTG GCC AGC TTTTT GCT GGC CAA TGC; ODN 9, ICB5 5′-flank, 5′-GAT AGA TTG GCC TTTTT GGC CAA TCT ATC; ODN 10, ICB5 3′-flank, 5′-GGA TTG GCA GTC TTTTT GAC TGC CAA TCC.

Melting experimental data were obtained on a Cary 3 spectrophotometer. The experiments with the oligomers were run in Phos 0 buffer (10 mM sodium phosphate and 1.58 mM EDTA, pH 6.2) at a ratio of 2.56 nmol of ligand to 0.852 nmol of DNA duplex. The total volume of each sample was diluted to 1.00 mL with the Phos 0 buffer. Samples were heated above their melting temperature (usually around 95 °C) and allowed to slowly cool to the starting temperature. The Cary 3 spectrophotometer collects absorbance values as a function of increasing temperature, and the data points are then stored and analyzed at the conclusion of the experiment. Averaged absorbance readings are taken every 0.5 °C for each sample. Once all of the data points were compiled, the data were analyzed by a statistical software package, KaleidaGraph. The T_M value for each run was determined as the maximum of the first derivative (δabsorbance/δtemperature versus temperature) of the results.

CD Titration Studies. The oligonucleotides used in these studies were identical to those used in the thermal denaturation studies. The oligomers (ICB1−3) were resuspended in TE buffer (10 mM Tris and 1 mM EDTA, pH 6.9) and subsequently diluted to 9 μM DNA hairpin by ∼100-fold with MES buffer [10 mM 2-(*N*-morpholino)ethanesulfonic acid, 200 mM NaCl, and 1 mM EDTA, pH 6.2] for direct use in circular dichroism experiments. Concentrated **JH-37** (>65 μM) was titrated into the cuvette with increasing mole ratios of 0.2:1−0.5:1 ligand to DNA hairpin until a ratio of 3:1 was reached. The experiments were carried out a ambient temperature in a 1 mm path length circular cuvette with a minimum required volume of 160 μL, and the data were averaged over six scans.

The height of the induced peak at ∼320 nm was normalized ($mdeg_x/mdeg_{max}$) and plotted versus the mole ratio, and the intersection of the linear regression fits of the data indicates the stoichiometry of the DNA:**JH-37** complex at equilibrium.

SPR and ITC Studies. (A) DNAs and Polyamides. The hairpin polyamide **JH-37** was used with ϵ_{312} = 56800 M^{-1} cm^{-1}, and the 5′-biotin-labeled DNA hairpins (for SPR) or nonlabeled hairpins (for ITC) were purchased with HPLC purification (Midland Certified Reagent Co., Midland, TX) and used without further purification. The DNA hairpins were used with ϵ_{260} = 9320 M^{-1} cm^{-1} bases (for ICB2) from the nearest neighbor calculations (*18*), and their structures are as follows: ICB2, 5′-biotin-CGA TTG GTT GTT TTT CAA

Scheme 1: Solution Phase Synthesis of **JH-37**

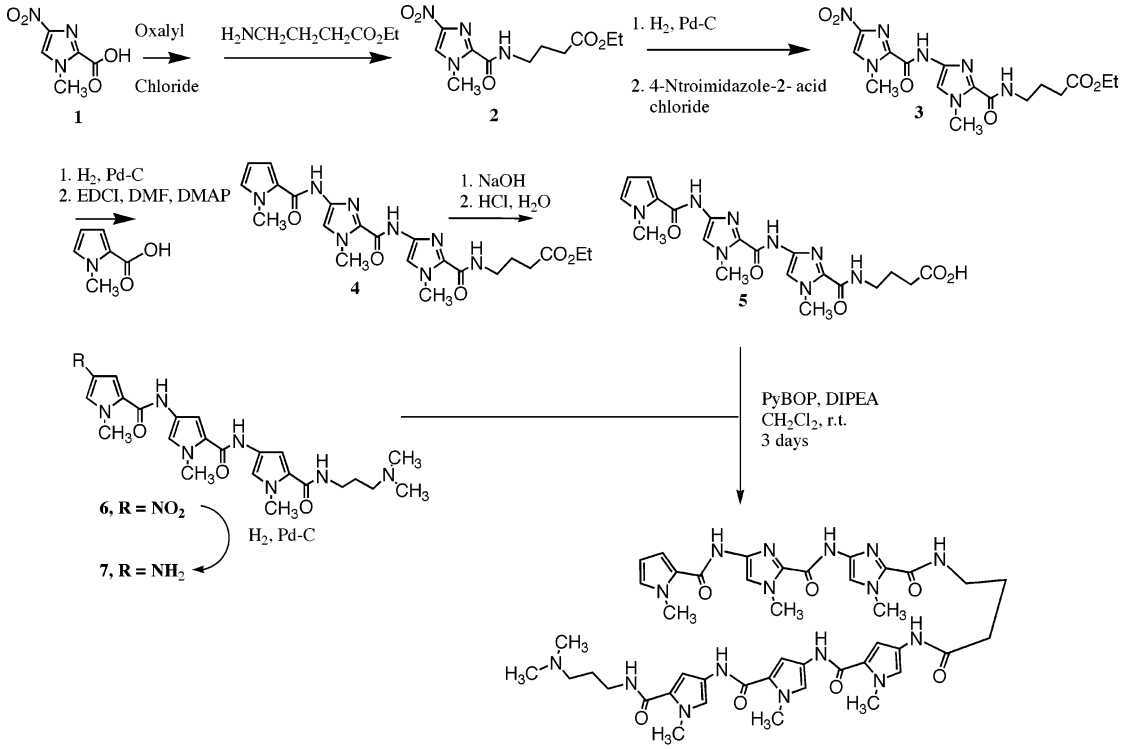

JH-37

CCA ATC G; ICB1, 5′-biotin-CGA TTG GCT GTT TTT CAG CCA ATC G; ICB2m, 5′-biotin-CGA TCG GTT GTT TTT CAA CCG ATC G; TGCA, 5′-biotin-GAA TGC ATT CTC TAA TGC ATT C. The MES buffer used in these experiments contained 0.010 M 2-(*N*-morpholino)ethanesulfonic acid (MES), 0.001 M EDTA, and 0.2 M NaCl, pH 6.25.

(B) Surface Plasmon Resonance (SPR). The experiments were performed on a BIACORE 3000 instrument, and BIACORE SA sensor chips were used for DNA immobilization (*19*−*21*). In brief, manual injections were used to immobilize samples of approximately 14 nM biotinylated DNA at a flow rate of 1 μL/min. The amount of DNA captured was about 400 RUs on each flow cell. One flow cell was left blank and used as reference. The sensorgrams for the interaction (resonance units, RU, versus time) were collected at 25 °C with a flow rate of 20 μL/min. The compound was dissolved in degassed MES buffer with 5×10^{-3} % (v/v) surfactant P20. This buffer was also used in surface regeneration. The data were processed with BIAevaluation software (Biacore AB, Uppsala, Sweden) and KaleidaGraph (Synergy Software, Reading, PA). The RU values were averaged over a 1 min time span in the steady-state response region and were converted to *r* (moles of compound bound per mole of DNA hairpin) for binding analysis. This was done by dividing the response units by the predicted RU_{max} as previously described using a refractive index increment ratio of 1.3 (*34*). The binding constants of the compounds were obtained from fitting a plot of *r* versus compound concentration. The plot was fitted with a one or two-site model (for a one-site model, $K_2 = 0$):

$$r = (K_1C_{free} + 2K_1K_2C^2_{free})/(1 + K_1C_{free} + K_1K_2C^2_{free})$$

Kinetic information was obtained by global fitting of the response units vs time with the BIAevaluation 3.0 program. The association and dissociation rate constants (k_a and k_d) were obtained by global fitting with a model with mass transport effects (*19*−*21*).

(C) Isothermal Titration Calorimetry (ITC). Calorimetric experiments were performed with a MicroCalorimeter VP-ITC (MicroCal, Northampton, MA). The instrument was electrically calibrated with heat pulses and chemically calibrated with these pairs of reagents: RNase A−2′-CMP, $BaCl_2$−18-crown-6, HCl−THAM (Aldrich Chemical Co., Milwaukee, WI). The values are in agreement with literature values (*22*). The experiments were conducted by injecting 3 μL aliquots of 0.05 mM ligand into 2 μM DNA hairpin in degassed MES buffer at 25 °C, 290 rpm, 1 s filter, 5 min initial delay, and 6 s injection time. Heats of dilution were subtracted from the data before fitting with a sequential binding site model using Microcal Origin version 5.0 (*23*).

RESULTS AND DISCUSSION

Synthesis. The synthesis of **JH-37** is described in Scheme 1. The products were characterized with FT-IR, 500 MHz ^{1}H NMR, and mass spectrometry (nominal and accurate mass measurements). Conversion of 1-methyl-4-nitroimidazole-2-carboxylic acid (**1**) to an acid chloride followed by coupling it with ethyl-β-alanine gave amide **2**, which we have previously reported (*24*). Reduction of the nitro group in amide **2** by catalytic hydrogenation followed by reaction of the amine with another molecule of imidazole acid chloride gave the dipeptide **3**. The nitro group in dipeptide **3** was reduced and coupled to 1-methylpyrrole-2-carboxylic acid in the presence of EDCI [1-ethyl-3-(3′-dimethylaminopropyl)-carbodiimide hydrochloride] and DMAP [4-(dimethylamino)-pyridine]. The reaction produced tripeptide **4**, which was hydrolyzed with sodium hydroxide to afford carboxylic acid **5**. Reduction of a tripyrroleamide **6** and condensation of the

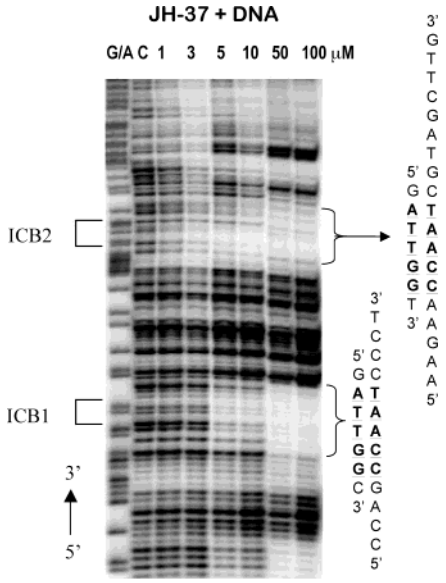

FIGURE 2: DNase I footprinting of **JH-37** using a 5′-^{32}P-radiolabeled probe corresponding to the topoisomerase IIα promoter. C represents a control for DNase I cleavage of the probe. Lane 1 contains the G-A sequencing lane, lane 2 contains the probe, and lanes 3−8 contain increasing concentrations of **JH-37** (1, 3, 5, 10, 50, and 100 μM). The ICB1 and ICB2 sites are indicated, and the brace denotes the footprint observed.

corresponding amine **7** (*25*) with acid **5** in the presence of PyBOP (benzotriazol-1-yloxytripyrrolidinophosphonium hexafluorophosphate) and DIPEA (diisopropylethylamine) gave the desired hairpin polyamide **JH-37** in 37% yield.

*DNase I Footprinting Studies on **JH-37**.* The sequence specificity of **JH-37** was investigated using DNase I footprinting studies, using a 479 bp 5′-^{32}P-radiolabeled fragment containing its promoter (Figure 2). At 5 μM **JH-37**, cleavage of the DNA by DNase I or footprints were apparent at ICB1 and ICB2 sequences. Unlike Hoechst 33342, **JH-37** produced protections only at the ICB sites, and none was seen at the other AT-rich sites that interacted with the Hoechst compound (*4*). At even higher concentrations of **JH-37** (50−100 μM), clear footprints were seen at 3′-GTTCGATGC**TAACC**AAGAA-5′ [corresponding to 5′-C(−118)-AAGCTACG**ATTGG**TTCTT(−100)-3′] and 3′-TCCC-**TAACC**GACC-5′ [corresponding to 5′-A(−72)GGG-**ATTGG**CTGG(−60)-3′]. The former footprint contains the embedded ICB2 sequence (bold), while the latter footprint contains the ICB1 site, which is also in bold. These results provide evidence that **JH-37** exhibits selectivity for the ICB sequences. The binding of **JH-37** to ICB1 is not totally surprising because this sequence is almost identical to that for ICB2,3 (5′-ATTGGC-3′ versus 5′-ATTGGT-3′, respectively). In these instances, the γ-butyrate linker which has low preference for an A·T over a G·C base pair resides over the 3′-C or 3′-T in these sequences (*12*, *26*−*28*).

Binding of **JH-37** to ICB sites and its ability to inhibit the binding of NF-Y were confirmed by electrophoretic mobility shift studies (data will be reported elsewhere). Briefly, these gel shift experiments were carried out using 5′-^{32}P-labeled oligonucleotides containing sequences of ICB1−4 found in the promoter. The probes were incubated with nuclear extracts (containing NF-Y) from confluent NIH 3T3 cells and with increasing concentration of **JH-37**. At about 5 μM, there was inhibition of NF-Y binding to the ICB2,3 sequences, but binding to ICB1 was also observed, albeit not as strongly.

*Biophysical Studies on **JH-37**.* Molecular biology experiments are powerful tools for studying biomolecular interactions, but they are generally limited in terms of providing critical thermodynamic and kinetic properties for the recognition processes. These physical factors permit the construction of quantitative structure−activity relationships that are critical for guiding our design of new polyamides with enhanced binding affinity and sequence specificity.

Thermal Denaturation Studies: Sequence Preference. Compounds that bind to DNA and stabilize the double helix raise the temperature needed for denaturation or melting of the duplex. The duplex unfolding can be followed through the associated hyperchromic effect at 260 nm. The ΔT_M values, derived from the difference in melting temperatures of the polyamide/DNA complex and DNA alone, provide a quick method for screening the binding affinity of **JH-37** for 10 different DNA hairpins given in the Experimental Procedures. Each DNA hairpin (ODN1−10) contains an ICB core and the appropriate 5′- or 3′-flanking base pairs. Treatment of the hairpin oligomers (0.9 μM, base pairs), representing ICB1−5, with 3 equiv of **JH-37** gave a range of ΔT_M values, with the highest degree of stabilization recorded for ICB2 and ICB3 (8−9 °C), over ICB1,4,5 (4−5 °C). These results corroborated the sequence preference of **JH-37** from the above footprinting experiments.

CD Titration Studies: Evidence of Minor Groove Binding and Stoichiometry. While thermal denaturation experiments are rapid and give useful information, they do not provide information regarding the mechanism of interactions between **JH-37** and the DNAs. Accordingly, a number of CD (circular dichroism) titration studies were carried out using 9.0 μM hairpin ICB1−3 sequences and **JH-37**, corresponding to specific polyamide/DNA ratios. The results depicted in Figure 3 clearly show **JH-37** to bind to the ICB2 and ICB3 sequences. Each titration experiment produced well-defined positive DNA-induced ligand bands at about 320 nm, which are diagnostic for small molecules binding in the minor groove of DNA (*29*). Furthermore, in each set of titration spectra, clear isodichroic points are apparent, indicating that **JH-37** binds to the oligomers through a single mechanism, presumably through noncovalent binding in the minor groove. CD experiments are also very useful in providing the stoichiometry of ligands binding to DNA. Plots of ellipticity of the DNA-induced ligand band versus the ratio of moles of polyamide to moles of DNA hairpins indicate that only one molecule of **JH-37** binds to DNA hairpins that contain one 5′-(A·T)GG sequence (this is within the 5′-ATTGG-3′ ICB sequence). ICB1 (3′- and 5′-flanks) and ICB3 (5′-flank), which contain two 5′-(A·T)GG sequences, gave a binding stoichiometry of 2. Our hairpin polyamide (**JH-37**) binds to 5′-TGG and 5′-AGG because the Py/Py pair at one end of the molecule (Figure 3C) is able to recognize an A·T or T·A base pair. Even though the CD data provided useful qualitative information concerning the binding of **JH-37** to the ICB-containing sequences, we needed to gain a deeper insight into the thermodynamic and kinetic factors that drive the sequence-specific molecular recognition process. Our goal is to use the physical information for the future design of compounds with superior DNA binding properties.

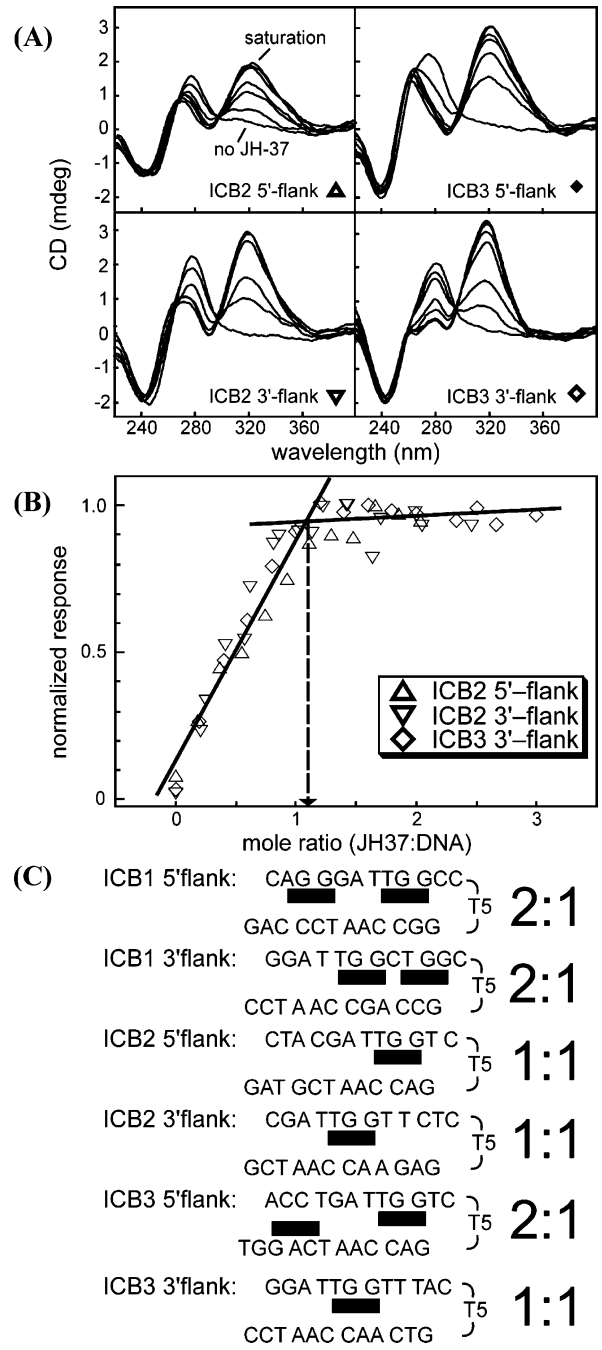

FIGURE 3: (A) CD titration studies of **JH-37** to ICB2 and ICB3. For the ICB2 5′-flank, the ratios of moles of **JH-37** to moles of DNA hairpins were 0, 0.18, 0.56, 0.74, 1.11, 1.48, and 2.04. The spectrum for DNA alone (i.e., no **JH-37**) and the spectrum when all binding sites on the DNA were bound with **JH-37** (i.e., saturation) are indicated. For the ICB2 3′-flank, the ratios were 0, 0.26, 0.57, 1.14, 1.42, and 2.00. For the ICB3 5′-flank, the ratios were 0, 0.6, 1.0, 1.6, 2.0, 2.5, and 3.0. For the ICB3 3′-flank, the ratios were 0, 0.2, 0.4, 0.8, 1.0, 1.4, 2.0, and 3.0. (B) Plot of normalized DNA-induced ellipticity at about 320 nm versus the ratio of moles of DNA hairpins. Triangles represent the titration of **JH-37** to the ICB2 5′-flank, inverted triangles represent **JH-37** plus the ICB2 3′-flank, and diamonds represent **JH-37** and the ICB3 3′-flank. (C) Models for the binding of **JH-37** to the ICB1−3 3′- and 5′-flanking sequences. The stacked heterocyclic system of **JH-37** recognizes (A·T)GG sites. Consequently, the ICB1 3′- and 5′-flanking sequences and the ICB3 5′-flank that contain two (A·T)GG sites gave a binding stoichiometry of 2, as indicated by the solid lines. The ICB2 3′- and 5′-flanking sequences and the ICB3 3′-flank, which contain only one (A·T)GG site, gave a binding stoichiometry of 1.

Biosensor−Surface Plasmon Resonance (SPR): Binding Strength, Stoichiometry, Specificity, and Kinetics. Surface plasmon resonance (SPR) has emerged as an excellent tool for studying small molecule−DNA interactions (*30*, *31*), particularly for compounds such as **JH-37** that have strong DNA interactions but weak spectroscopic signals. This method permits the measurement of both thermodynamics (binding constant and $\Delta G°$), binding stoichiometry, and kinetic constants (k_a and k_d for association and dissociation, respectively) of ligand−DNA interactions in a single experiment. These are key physical parameters for the design of compounds that could inhibit the function of transcription factors in cells. These compounds must have large binding constants ($>10^6$ M^{-1}) to compete with transcription factors for their promoter sequences. It is known that a slow rate of dissociation (k_d) is crucial for providing the compound with sufficient resident time within the DNA to impart its transcriptional inhibitory activity (*32*, *33*). This contention is reasonable because the binding constant is equal to the ratio of k_a/k_d.

The interactions of **JH-37** with ICB2 and several modified DNA sequences, whose structures are given in the Experimental Procedures, were investigated by biosensor−SPR methods with immobilized DNA hairpin duplexes. The ICB2 oligomer contains a 5′-AATTGGT core sequence, and the modified sequences contain either an ICB1 site (5′-ATTGGC), an ICB2 mutant (5′-ATCGGT, ICB2m), or a non-ICB sequence (5′-ATGCAT or TGCA). The results from these studies are given in Figure 4, and example sets of sensorgrams for addition of **JH-37** to ICB2 and the TGCA sequence are shown in parts A and B of Figure 4, respectively. As can be seen in the figure, the initial rate of binding of **JH-37** increases with increasing concentration, as expected for a bimolecular process, and the binding reaction reaches a steady-state plateau for all DNA sequences in approximately 100 s or less. In contrast, the observed rate constant for dissociation of **JH-37** is independent of concentration, in agreement with the expected unimolecular, first-order process. Binding constants were determined from the RU values at steady state and the concentration of **JH-37** in the flow solution (C_{free}). The RU values at saturation can be determined by direct calculation (*34*) or by fitting the response units (RU) versus C_{free} values. The calculated and experimental values of RU_{max} for these titrations agree closely and predict a single strong binding site on all ICB2 duplexes, as expected from their sequences. The RU values were converted to r (where r is the moles of **JH-37** bound per mole of hairpin duplex; $r = RU/RU_{max}$) and plotted versus C_{free} (Figure 4C). The r versus C_{free} results were fitted with a model of one **JH-37** binding site on each duplex. The fits were slightly improved by including a second, much weaker binding site with a K that is approximately 100 times lower than for the strong binding site. The nature of the second interaction is not known, but such weak interactions are characteristic of nonspecific electrostatic binding of cations to DNA (*31*). The binding constants for the strong, specific site were fitted accurately and are collected in Table 1. As expected, **JH-37** binds quite strongly to ICB2 with a K that is 4−5-fold greater than for ICB1, over 50 times larger than for ICB2m and approximately 10 times larger than for TGCA.

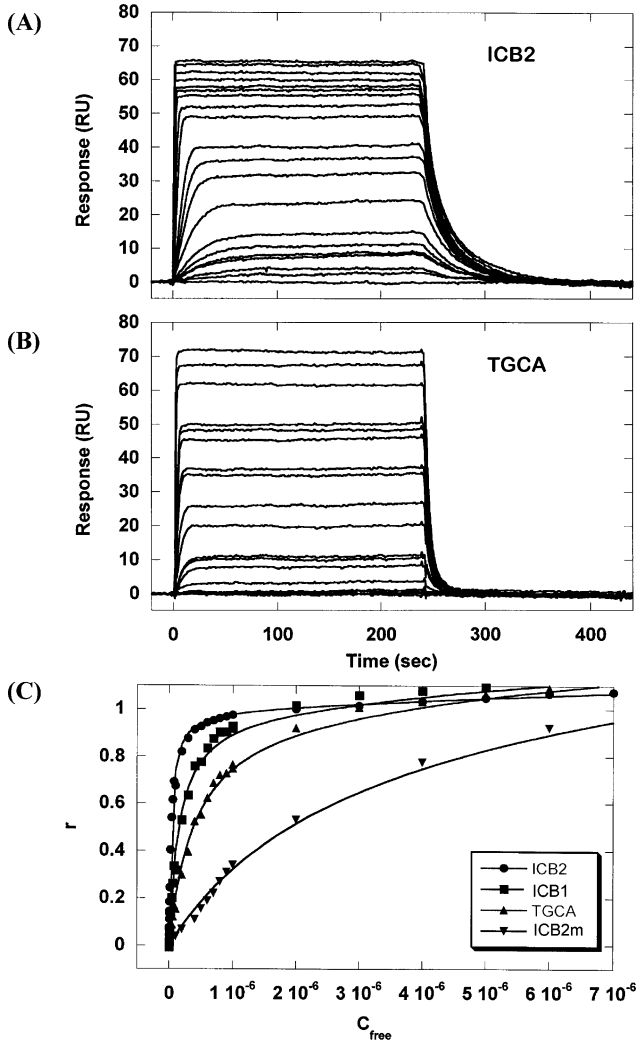

FIGURE 4: SPR sensorgrams for the binding of **JH-37** to ICB2 (A) and TCGA (B). (C) Plot of response units (RU) obtained from SPR studies versus concentration of **JH-37** in the flow solution (C_{free}).

Table 1: Summary of Binding Constants for **JH-37**: K (M^{-1}), k_a(M^{-1} s^{-1}), and k_d (s^{-1})

	SPR		
DNA	steady state[a]	kinetics[b]	ITC[c]
ICB2	2.8×10^7	$k_a/k_d = 3.6 \times 10^7$ $k_a = 3.3 \times 10^6$ $k_d = 9.0 \times 10^{-2}$	2.7×10^7
ICB1	6.5×10^6	$k_a/k_d = 7.2 \times 10^6$ $k_a = 5.9 \times 10^6$ $k_d = 7.8 \times 10^{-1}$	
ICB2m	4.3×10^5		
TGCA	2.5×10^6		

[a] The binding constants were obtained from steady-state fittings using a two-site interactive binding model. The fitting errors are less than 10%. [b] The rate constants obtained from kinetic fitting include mass transport effects. The fitting errors are less than 15%. [c] The primary binding constant was obtained from fitting ITC data with a two-site sequential binding model. The observed change in enthalpy is -5.7 ± 0.1 kcal/mol. The fitting error is less than 25%.

The rates of **JH-37** binding to the DNA hairpins can be determined by fitting both the association and dissociation reactions in sets of sensorgrams, such as those in Figure 4. The kinetic constants for binding of ICB2m and TGCA were too fast to be determined by SPR, but for ICB2 and ICB1

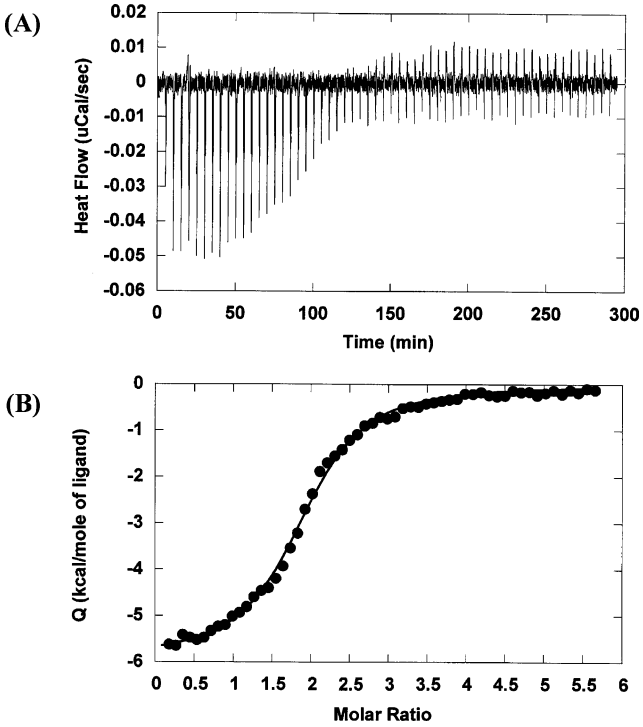

FIGURE 5: (A) Plot of the ITC titration of heat versus injection of **JH-37** to ICB2. (B) Heat/mol versus titration molar ratio.

the constants were determined by global fitting of sensorgrams (Table 1). The equilibrium constants can be estimated from the k_a/k_d ratios and they are in agreement with those determined by steady-state fitting (Table 1). The k_a values for **JH-37** binding to ICB2 and ICB1 are close, and the difference in dissociation constants accounts for most of the difference in the K values of **JH-37** for these two sequences. Although the kinetic constants for **JH-37** binding to ICB2m and TGCA could not be determined accurately under our conditions, it is clear from examination of the sensorgrams that the k_d values for ICB2m and TGCA are significantly greater than for ICB2. These results indicate that the kinetic and mechanistic basis that dictates the binding specificity for **JH-37** with the modified sequences is different than with cognate recognition sequences.

Isothermal Titration Calorimetry (ITC): Thermodynamic Basis of the Interaction. To develop a better understanding of the energetic details for the interaction of **JH-37** as well as polyamide hairpins in general with DNA, the binding of **JH-37** to ICB2 was studied with ITC methods. An example ITC titration of heat versus injection of **JH-37** into ICB2 along with a binding plot of observed heat/mole (Q) versus titration molar ratio is shown in Figure 5. Because ITC titrations are done at much higher concentrations of **JH-37** to DNA, the weaker, secondary binding, which could hardly be observed by SPR methods, becomes more apparent in calorimetry experiments (Figure 5). The ITC results also fit quite well with a model that has one strong and one weak binding site for **JH-37** on ICB2, and the binding affinity for the strong binding site is reported in Table 1. The $\Delta H°$ value determined from the fit for **JH-37** binding to the ICB2 sequence is -5.7 kcal/mol. The K and $\Delta H°$ results for binding of **JH-37** to ICB 2 allow calculation of $\Delta G° = -10.1$ kcal/mol and $T\Delta S° = 4.4$ kcal/mol ($\Delta G° = -RT \ln K$ and $T\Delta S° = -\Delta G° + \Delta H°$). These results clearly show

that both the enthalpy and entropy make significant contributions to the very favorable $\Delta G°$ for binding of **JH-37** to ICB2 at 25 °C.

CONCLUSIONS

The results generated from the above studies illustrate that hairpin imidazole−pyrrole polyamides can be designed to bind specific ICB-containing DNA sequences. Even though the six-heterocycle hairpin polyamide **JH-37** binds to five base pairs, it gave sufficient affinity and selectivity for ICB2 and ICB3, as well as ICB1. It did not bind to AT-rich sequences such as Hoechst 33342. This is a significant finding because the results from electrophoretic mobility shift studies showed **JH-37** to inhibit the binding of NF-Y to ICB1-, ICB2-, and ICB3-containing oligonucleotides (data not shown). Furthermore, it is worthy to mention that the binding of NF-Y to an ICB site is about 10^{10} M^{-1}, one of the strongest binders among transcription factors (*35*). These findings are consistent with what was found in Dervan's group (*36*−*38*). Hairpin polyamides that recognize six to seven base pairs are able to enter cells and affect specific gene expression, but larger hairpins that target longer sequences of DNA have not had success in cellular experiments. For instance, polyamides that target nine base pair sequences in the human *HER2/neu* gene gave excellent activity in cell-free systems (*39*), but the compounds showed no activity in vivo (*40*). It has recently been found that most of the larger polyamides tend to concentrate in the cytoplasm of cells, and only in certain leukemia cells (CEM) do these compounds readily enter the nucleus (*41*, *42*). The development of novel gene-based therapeutic compounds would thus require the consideration of an alternative strategy. Instead of focusing on 15−16 contiguous base pairs, which statistically define a unique sequence in the human genome, one should consider targeting shorter sequences that are adjacent to each other in an array within a promoter (*12*, *43*, *44*). For example, one could design a molecule that interacts simultaneously with all or several of the five ICB sites within the promoter of the topoisomerase IIα gene. An ideal test for this strategy will be to use **JH-37**, which binds to five base pairs, as a template for the design of novel derivatives for recognition of the ICB sequences. To our knowledge, this is the first report that systematically evaluates such a strategy for the design of molecules that target an array of shorter sequences within the promoter region of a gene. With the evidence presented for the binding of **JH-37** to ICB sequences within the topoisomerase IIα promoter, studies to investigate the biological properties are in progress. The biological experiments include studies on **JH-37** inhibition of the binding of NF-Y to specific ICB sequences, penetration of the agent into the nucleus of cells and binding to ICB sites in nuclear DNA, and modulation in the expression of the topoisomerase IIα gene. The results from these studies will be reported in due course.

REFERENCES

1. Isaacs, R. J., Harris, A. L., and Hickson, I. D. (1996) Regulation of the human topoisomerase IIα gene promoter in confluence-arrested cells, *J. Biol. Chem. 271*, 16741−16747.
2. Wang, J. C. (1996) DNA topoisomerases, *Annu. Rev. Biochem. 65*, 635−692.
3. Wang, H., Jiang, Z., Wong, Y. W., Dalton, W. S., Futscher, B. W., and Chan, V. T. (1997) Decreased CP-1 (NF-Y) activity results in transcriptional down-regulation of topoisomerase IIα in a doxorubicin-resistant variant of human multiple myeloma RPMI 8226, *Biochem. Biophys. Res. Commun. 237*, 217−224.
4. Tolner, B., Hartley, J. A., and Hochhauser, D. (2001) Transcriptional regulation of topoisomerase IIα at confluence and pharmacological modulation of expression by bis-benzimidazole drugs, *Mol. Pharmacol. 59*, 699−706.
5. Adachi, N., Nomoto, M., Kohno, K., and Koyama, H. (2000) Cell-cycle regulation of the DNA topoisomerase IIα promoter is mediated by proximal CCAAT boxes: possible involvement of acetylation, *Gene 245*, 49−57.
6. Ronchi, A., Bellorini, M., Mongelli, N., and Mantovani, R. (1995) CCAAT-box binding protein NF-Y (CBF, CP1) recognizes the minor groove and distorts DNA, *Nucleic Acids Res. 23*, 4565−4572.
7. Mantovani, R. (1999) The molecular biology of the CCAAT-binding factor NF-Y, *Gene 239*, 15−27.
8. Suhkai, M., and Piquette-Miller, M. (2000) Regulation of the multidrug resistant genes by stress signals, *J. Pharm. Pharm. Sci. 3*, 268−280.
9. Scotto, K. W., and Johnson, R. A. (2001) The regulation of the multidrug resistant gene Mdr1: a therapeutic target, *Mol. Interventions 1*, 117−125.
10. Schinkel, A. H. (1997) The physiological function of drug-transporting P-glycoproteins, *Semin. Cancer Biol. 8*, 161−170.
11. Tomida, A., and Tsuruo, T. (1999) Drug resistance mediated by cellular stress response to the microenvironment of solid tumors, *Anti-Cancer Drug Des. 14*, 169−177.
12. Dervan, P. B., and Edelson, B. S. (2003) Recognition of the DNA minor groove by pyrrole-imidazole polyamides, *Curr. Opin. Struct. Biol. 13*, 284−299.
13. Gottesfeld, J. M., Turner, J. M., and Dervan, P. B. (2000) Chemical approaches to control gene expression, *Gene Expression 9*, 77−91.
14. Kopka, M. L., Goodsell, D. S., Han, G. W., Chiu, T. K., Lown, J. W., and Dickerson, R. E. (1997) Defining GC-specificity in the minor groove: side-by-side binding of the di-imidazole lexitropsin to CATGGCCATG, *Structure 5*, 1033−1046.
15. Yang, X.-L., Kaenzig, C., Lee, M., and Wang, A. H.-J. (1999) Binding of AR-1−144, a triimidazole DNA minor groove binder, to CCGG sequence analyzed by NMR spectroscopy, *Eur. J. Biochem. 263*, 646−655.
16. Yang, X.-L., Hubbard, R. B., IV, Lee, M., Tao, Z.-H., Sugiyama, H., and Wang, A. H.-J. (1999) Imidazole-imidazole pair as a minor groove recognition motif for T:G mismatched base pairs, *Nucleic Acids Res. 27*, 4183−4190.
17. Lacy, E. R., Le, N. M., Price, C. A., Lee, M., and Wilson, D. W. (2002) Influence of a terminal formamido group on the sequence recognition of DNA by polyamides, *J. Am. Chem. Soc. 124*, 2153−2165.
18. Fasman, G. D., Ed. (1975) *Handbook of Biochemistry and Molecular Biology: Nucleic Acids*, 3rd ed., Vol. 1, CRC Press, Cleveland, OH.
19. BIACORE (1997) *BIAevaluation version 3.0: Software Handbook*, Biacore AB, Uppsala, Sweden.
20. BIACORE (1994) *BIAapplications Handbook*, Biacore AB, Uppsala, Sweden.
21. Myszka, D. G., He, X., Dembo, M., Morton, T. A., and Goldstein, B. (1998) Extending the range of rate constants available from BIACORE: interpreting mass transport-influenced binding data, *Biophys. J. 75*, 583−594.
22. Horn, J. R., Russell, D., Lewis, E. A., and Murphy, K. P. (2001) van't Hoff and calorimetric enthalpies from isothermal titration calorimetry: are there significant discrepancies?, *Biochemistry 40*, 1774−1778.
23. Microcal (1997) *Microcal Origin User's Manual. Vol. Version 5*, Microcal Software, Inc., Northampton, MA.
24. Wyatt, M. D., Garbiras, B. J., Lee, M., Forrow, S. M., and Hartley, J. A. (1994) Synthesis and DNA binding properties of a series of N to C linked and imidazole containing analogues of distamycin, *Bioorg. Med. Chem. Lett. 4*, 801−806.
25. Brooks, N., Hartley, J. A., Simpson, J. E., Jr., Wright, S. R., Woo, S., Centioni, S., Fontaine, M. D., McIntyre, T. E., and Lee, M. (1997) Structure−activity relationship of a series of C-terminus modified aminoalkyl, diaminoalkyl- and anilino-containing analogues of the benzoic acid mustard distamycin derivative tallimustine: synthesis, DNA binding and cytotoxic studies, *Bioorg. Med. Chem. 5*, 1497−1507.

26. Dervan, P. B., and Burlii, R. W. (1999) Sequence specific DNA recognition by polyamides, *Curr. Opin. Chem. Biol. 3*, 688−693.
27. Wemmer, D. E., and Dervan, P. B. (1997) Targeting the minor groove of DNA, *Curr. Opin. Struct. Biol. 7*, 355−361.
28. Wemmer, D. E. (2000) Design sequence-specific minor groove ligands, *Annu. Rev. Biophys. Biomol. Struct. 29*, 439−461.
29. Rodger, L. R., and Norden, B. (1992) The CD of ligand-DNA systems. 2. poly(dA-dT) B-DNA, *Biopolymers 32*, 1201−1214.
30. Wang, L., Bailly, C., Kumar, A., Ding, D., Bajic, M., Boykin, D. W., and Wilson, D. W. (2000) Specific molecular recognition of mixed nucleic acid sequences: an aromatic dication that binds in the DNA minor groove as a dimer, *Proc. Natl. Acad. Sci. U.S.A. 97*, 12−16.
31. Wilson, D. W. (2002) Analyzing biomolecular interactions, *Science 295*, 2103−2105.
32. Paal, K., Baeuerle, P. A., and Schmitz, L. (1997) Basal transcription factors TBP and TFIIB and the viral coactivator E1A 13S bind with distinct affinities and kinetics to the transactivation domain of NF-κB p65, *Nucleic Acids Res. 25*, 1050−1055.
33. Ptashne, M., and Gann, A. (2001) *Genes and Signals*, 1st ed., Cold Spring Harbor Laboratory, Cold Spring Harbor, NY.
34. Davis, T. M., and Wilson, W. D. (2000) Determination of the refractive index increments of small molecules for correction of surface plasmon resonance data, *Anal. Biochem. 284*, 348−353.
35. Kim, C. G., and Sheffery, M. (1990) Physical characterization of the purified CCAAT transcription factor, α-CP1, *J. Biol. Chem. 265*, 13362−13369.
36. Gottesfeld, J. M., Neely, L., Trauger, J. W., Baird, E. E., and Dervan, P. B. (1997) Regulation of gene expression by small molecules, *Nature 387*, 202−205.
37. Dickinson, L. A., Gulizia, R. J., Trauger, J. W., Baird, E. E., Mosier, D. E., Gottesfeld, J. M., and Dervan, P. B. (1998) Inhibition of RNA polymerase II transcription in human cells by synthetic DNA-binding ligands, *Proc. Natl. Acad. Sci. U.S.A. 95*, 12890−12895.
38. Coull, J. J., He, G., Melander, C., Rucker, V. C., Dervan, P. B., and Margolis, D. M. (2002) Targeted derepression of the human immunodeficiency virus type 1 long terminal repeat by pyrrole-imidazole polyamides, *J. Virol. 76*, 12349−12354.
39. Chiang, S.-Y., Burli, R. W., Benz, C. C., Gawron, L., Scott, G. K., Dervan, P. B., and Beerman, T. A. (2000) Target the Ets binding site of the HER2/neu promoter with pyrrole-Imidazole polyamides, *J. Biol. Chem. 275*, 24246−24254.
40. Dervan, P. B. (2001) Molecular recognition of DNA by small molecules, *Bioorg. Med. Chem. 9*, 2215−2235.
41. Belitsky, J. M., Leslie, S. J., Arora, P. S., Berman, T. A., and Dervan, P. B. (2002) Cellular uptake of *N*-methylpyrrole/*N*-methylimidazole polyamide-dye conjugates, *Bioorg. Med. Chem. 10*, 3313−3318.
42. Crowley, K. S., Phillion, D. P., Woodard, S. S., Schweitzer, B. A., Singh, M., Shahany, H., Burnette, B., Hippenmeyer, P., Heitmeier, M., and Bashkin, J. K. (2003) Controlling the intracellular localization of fluorescent polyamide analogues in cultured cells, *Bioorg. Med. Chem. Lett. 13*, 1565−1570.
43. Helene, C. (1998) Reading the minor groove, *Nature 391*, 436−438.
44. Neidle, S. (2001) DNA minor-groove recognition by small molecules, *Nat. Prod. Rep. 18*, 291−309.

BI048785Z